Paper:

Analytical Prediction of Part Dynamics for Machining Stability Analysis

Salih Alan*, Erhan Budak, and H. Nevzat Özgüven***

*Department of Mechanical Engineering, Middle East Technical University
06531 Ankara, Turkey
**Faculty of Engineering and Natural Sciences, Sabanci University
Orhanli, Tuzla, 34956 Istanbul, Turkey
E-mail: ebudak@sabanciuniv.edu
[Received December 18, 2009; accepted January 21, 2010]

An analytical procedure is developed to predict workpiece dynamics in a complete machining cycle in order to obtain frequency response functions (FRF), which are needed in chatter stability analyses. For this purpose, a structural modification method that is an efficient tool for updating FRFs is used. The mass removed by machining is considered to be a structural modification in order to determine the FRFs at different stages of the process. The method is implemented in a computer code and demonstrated on different geometries. The predictions are compared and verified by FEA. Predicted FRFs are used in chatter stability analyses, and the effect of part dynamics on stability is studied. Different cutting strategies are compared for increased chatter-free material removal rates considering part dynamics.

Keywords: chatter stability, part dynamics, structural modification

1. Introduction

Self-excited chatter vibrations in machining result from dynamic interactions between cutting tool and workpiece which may yield instability. Chatter causes poor surface finish, increased tool wear, damage to the machine tool and reduced productivity. Previous research indentified regenerative mechanism as the main source of chatter. The regenerative chatter can be explained as the vibrations induced by the phase shift between the waves generated in successive passes on the same surface [1, 2].

The theory of chatter in metal cutting was established by Tobias and Fishwick [3], and Tlusty and Polacek [4]. Later, the regenerative effect was modeled using the feedback control theory by Merritt [5]. Application of the receptance function to chatter prediction was offered by Tlusty [6]. The stability of milling is more complicated than orthogonal cutting due to the tool rotation, as this results in varying dynamics. Minis and Yanushevski [7] formulated the chatter in milling using Floquet's theorem and Fourier series and determined the stability limits numerically using the Nyquist stability criterion. By extending this approach, Budak and Altintas [8, 9] presented an analytical method for the stability prediction of milling. This method can be used to generate stability diagrams very efficiently.

Stability diagrams can be used effectively as a remedy for the chatter problem. In these diagrams, stable cutting depths are calculated using chatter models for different spindle speeds [1–9]. In the generation of stability diagrams, in addition to the chatter stability model, the total dynamic response at the cutting point, which includes tool point and part FRFs, must be known. The tool point FRF can be obtained by analytical methods or by experimental techniques. The application of receptance coupling techniques in the prediction of tool point FRF by combining tool and spindle point FRFs was first proposed by Schmitz et al. [10, 11]. This approach was later extended by Ertürk et al. [12–14]. They considered the Timoshenko beam model for the tool as well as contact dynamics at the interfaces and bearing support for increased accuracy. Experimental modal analysis can also be used to obtain tool dynamics.

For a flexible workpiece, FRFs of the part must be known for all stages of the machining cycle. Part dynamics prior to and after machining can be determined by experimental techniques or FEA. However, it would not be practical to use these methods for each stage of manufacturing because the part geometry, and thus the dynamics, varies continuously. The effect of the workpiece dynamics on chatter has been investigated by several researchers. Bravo et al. [15] and Thevenot et al. [16, 17] demonstrated that for thin-walled structures, part dynamics affects stability. They proposed the three-dimensional stability lobe diagram, the third dimension being the steps of the machining process or the tool position. The stability lobe diagrams for the intermediate stages of machining are plotted to obtain the 3D stability diagram. Le Lan et al. [18] used the finite element method to determine the stable depths of cut over a machining process and showed them on a stability map. A model considering the effect of part dynamics during milling was developed by Mañé et al. [19]. They optimized productivity by controlling the spindle speed during machining. Weinert et al. [20] studied the five-axis milling process in a time do-

main and modeled the workpiece using FEA. The material removal effect was introduced to chatter stability by Atlar et al. [21]. They modeled the workpiece as a beam considering changes in its dynamics and, therefore, the chatter stability as the workpiece is machined.

In this study, a structural modification technique is employed to predict the part dynamics during a complete machining cycle. In the method applied, the effect of removed material on the workpiece dynamics is considered. Based on the practical methodology presented, chatter stability analysis and predictions can be performed more accurately by considering the complete structural dynamics of a machining system. Özgüven [22] developed an exact and general method for structural modifications using FRFs. The method is applicable even for cases with additional degrees of freedom due to modification. The input for the method is the FRFs of the original system and the dynamic properties of the modifying structure. The FRFs of the modified structure are obtained as the output of the method at each machining step.

2. Chatter Stability

The limiting depth of cut for an orthogonal cutting process is given by Tlusty [2] as:

$$b_{\lim} = \frac{-1}{2 \cdot K_s \cdot \mathrm{R_e}\left(G(\omega)\right)} \quad . \quad . \quad . \quad . \quad . \quad . \quad . \quad . \quad . \quad (1)$$

where K_s is the cutting force coefficient in the chip direction relating the cutting force and the cutting area, and $G(\omega)$ is the FRF of the system. If the part dynamics is neglected, then the tool point FRF is directly taken as $G(\omega)$. However; if the flexibility of the workpiece is considered, the FRF of the system is calculated by the addition of the tool point FRF and the workpiece FRF at the contact position [21]:

$$[G(\omega)] = \left[G_{tool}(\omega) + G_{workpiece}(\omega)\right] \quad . \quad . \quad . \quad (2)$$

The analytical milling stability limit is given by Budak and Altintas [8, 9] as

$$a_{\lim} = -\frac{2\pi\Lambda_R}{NK_t}\left(1+\kappa^2\right) \quad . \quad . \quad . \quad . \quad . \quad . \quad . \quad . \quad . \quad (3)$$

where N is the number of cutting teeth on the tool, and Λ_R is the real part of the eigenvalue of the dynamic cutting system, and can be determined from the following expressions [8]:

$$\Lambda = -\frac{1}{2a_0}\left(a_1 \pm \sqrt{a_1^2 - 4a_0}\right) \quad . \quad . \quad . \quad . \quad . \quad . \quad (4)$$

where

$$\begin{aligned} a_0 &= G_{xx}(i\omega_c)G_{yy}(i\omega_c)(\alpha_{xx}\alpha_{yy} - \alpha_{xy}\alpha_{yx}) \\ a_1 &= \alpha_{xx}G_{xx}(i\omega_c) + \alpha_{yy}G_{yy}(i\omega_c) \end{aligned} \quad . \quad . \quad (5)$$

Here, G_{xx} and G_{yy} represent the sum of the tool point and workpiece FRFs in the x and y directions, respectively, as defined in Eq. (2). κ is the ratio of the imaginary and the real parts of the eigenvalue:

$$\kappa = \frac{\Lambda_I}{\Lambda_R} = \frac{\sin\omega_c T}{1-\cos\omega_c T} \quad . \quad . \quad . \quad . \quad . \quad . \quad . \quad . \quad . \quad (6)$$

Eq. (6) can be solved to obtain a relation between the chatter frequency and the spindle speed [8, 9] as follows:

$$\begin{aligned} &\omega_c T = \varepsilon + 2k\pi,\ \varepsilon = \pi - 2\psi, \\ &\psi = \tan^{-1}\kappa,\ n = \frac{60}{NT} \end{aligned} \quad . \quad . \quad . \quad . \quad . \quad . \quad . \quad . \quad . \quad (7)$$

where ε is the phase difference between the inner and outer modulations, k is an integer corresponding to the number of vibration waves within a tooth period, and n is the spindle speed (rpm). Therefore, for a given cutting geometry, cutting force coefficients, tool and workpiece FRFs, and a chatter frequency ω_c; Λ_I and Λ_R can be determined from Eq. (4) and can be used in Eqs. (7) and (3) to determine the corresponding spindle speed and the stability limit. When this procedure is repeated for a range of chatter frequencies and number of vibration waves, k, the stability lobe diagram for a milling system is obtained.

3. Prediction of Part Dynamics

3.1. Theoretical Background

In this section, the structural modification method with additional degrees of freedom will be introduced. The method applied is the Matrix Inversion Method, which is an FRF-based structural modification method developed by Özgüven [22]. Using the FRFs of the original system and the dynamic structural matrix of the modifying system, the FRFs of the modified system are calculated. Two different formulations are given in this method. The first one is applicable to structural modification without adding new degrees of freedom. The second one is for the systems which have additional degrees of freedom due to the modification. In this work, structural modification with additional degrees of freedom is used since degree of freedom change is necessary to model the material removal in machining steps.

The formulation of the structural modification with additional degrees of freedom is given below. The equation of motion for a dynamic system can be written as:

$$[M]\{\ddot{x}\} + i[H]\{\dot{x}\} + [K]\{x\} = \{F\} \quad . \quad . \quad . \quad . \quad . \quad (8)$$

In the above equation, $[M]$, $[H]$, and $[K]$ are the mass, structural damping, and stiffness matrices of the system, respectively. $\{F\}$ and $\{x\}$ vectors are the generalized force and coordinate vectors. The response $\{x\}$ of the system to a harmonic force $\{F\}$ with frequency ω can be expressed as:

$$\{x\} = \left[[K] - \omega^2[M] + i[H]\right]^{-1}\{F\} \quad . \quad . \quad . \quad . \quad . \quad (9)$$

The receptance matrix, $[\alpha]$, is defined by:

$$[\alpha] = \left[[K] - \omega^2[M] + i[H]\right]^{-1} \quad . \quad . \quad . \quad . \quad . \quad . \quad . \quad (10)$$

A structural modification to the original structure may

be represented by the modification matrices, $[\Delta M]$, $[\Delta H]$ and $[\Delta K]$. The dynamic structural modification matrix, $[D]$, can be written as:

$$[D] = [\Delta K] - \omega^2 [\Delta M] + i [\Delta H] \quad \ldots\ldots (11)$$

The receptance matrix, $[\gamma]$, of the modified structure is in the form of:

$$[\gamma] = [[[K] + [\Delta K]] - \omega^2 [[M] + [\Delta M]] + i [[H] + [\Delta H]]]^{-1} . \quad (12)$$

The coordinates of the modified structure can be divided into three groups. The first group, (a), involves the unmodified coordinates of the original structure. The second group, (b), is the group of coordinates which are contained by both the original and the modifying structures. The coordinates in the third group, (c), are the ones which belong only to the modifying structure. Using this classification, Eqs. (10) and (12) can be rewritten as follows:

$$[\alpha]^{-1} = \begin{bmatrix} \alpha_{aa} & \alpha_{ab} \\ \alpha_{ba} & \alpha_{bb} \end{bmatrix}^{-1} = [K] - \omega^2 [M] + i [H] \quad (13)$$

$$\begin{bmatrix} \gamma_{aa} & \gamma_{ab} & \gamma_{ac} \\ \gamma_{ba} & \gamma_{bb} & \gamma_{bc} \\ \gamma_{ca} & \gamma_{cb} & \gamma_{cc} \end{bmatrix}^{-1} = \begin{bmatrix} [\alpha]^{-1} & 0 \\ & 0 \\ 0 \quad 0 & 0 \end{bmatrix} + \begin{bmatrix} 0 & 0 & 0 \\ 0 & & \\ 0 & [D] & \end{bmatrix} . \quad (14)$$

Note that in the above equations, α_{ij} and γ_{ij} are submatrices of $[\alpha]$ and $[\gamma]$, respectively. After some matrix manipulations, the parts of the receptance matrix of the modified structure are obtained as:

$$\begin{bmatrix} \gamma_{ba} \\ \gamma_{ca} \end{bmatrix} = \left[\begin{bmatrix} I & 0 \\ 0 & 0 \end{bmatrix} + \begin{bmatrix} \alpha_{bb} & 0 \\ 0 & I \end{bmatrix} \cdot [D] \right]^{-1} \begin{bmatrix} \alpha_{ba} \\ 0 \end{bmatrix} \quad (15)$$

$$\begin{bmatrix} \gamma_{bb} & \gamma_{bc} \\ \gamma_{cb} & \gamma_{cc} \end{bmatrix} = \left[\begin{bmatrix} I & 0 \\ 0 & 0 \end{bmatrix} + \begin{bmatrix} \alpha_{bb} & 0 \\ 0 & I \end{bmatrix} \cdot [D] \right]^{-1} \begin{bmatrix} \alpha_{bb} & 0 \\ 0 & I \end{bmatrix} \quad \ldots\ldots (16)$$

$$[\gamma_{aa}] = [\alpha_{aa}] - \begin{bmatrix} \alpha_{ab} & \vdots & 0 \end{bmatrix} [D] \begin{bmatrix} \gamma_{ba} \\ \gamma_{ca} \end{bmatrix} \quad . . (17)$$

$$\begin{bmatrix} \gamma_{ab} & \vdots & \gamma_{ac} \end{bmatrix} = \begin{bmatrix} \alpha_{ab} & \vdots & 0 \end{bmatrix} \left[[I] - [D] \begin{bmatrix} \gamma_{bb} & \gamma_{bc} \\ \gamma_{cb} & \gamma_{cc} \end{bmatrix} \right] \quad . (18)$$

In the above formulation only a single matrix inversion is necessary. The order of this matrix is equal to the degree of freedom of the modifying structure, and it is generally much less than the degree of freedom of the modified structure. Note that the computational effort for matrix inversion becomes extremely high if the size of the matrix increases. Therefore, this method brings computational efficiency for local modifications.

The formulation described above is implemented in Matlab software. In the program, first of all $[\alpha]$ and $[D]$ are re-organized for matrix operations by identifying the intersecting nodes. The elements of $[\alpha]$ for the coordinates on the intersecting nodes must be on the lowermost rows and rightmost columns. Similarly, the elements related to the intersecting coordinates of the $[D]$ matrix must be on the topmost rows and leftmost columns. Then, Eqs. (15) through (18) are used to calculate the components of the FRF of the modified structure, $[\gamma]$.

3.2. Workpiece Dynamics Prediction Procedure

In the procedure implemented, FRFs of the workpiece at different machining stages are calculated based on its FRF at the final stage of machining, i.e. the finished geometry modeled with FEA using Ansys software, and by using the formulation given in section 3.1. The whole procedure can be divided into three steps: geometric and FE modeling, modal analysis and FRF extraction, and structural modification and FRF prediction.

The part geometry must be defined for each stage of the machining process in which its dynamics is required. The volume removed between two successive stages is modeled separately. The geometry of the workpiece can be modeled by CAD software whereas dynamic analysis can be done by FEA software. In addition, the dynamics at intermediate machining stages can be predicted using the structural modification formulation presented. The unmachined model is meshed using three-dimensional solid elements. The data obtained by meshing are saved to be used in the following steps. These data include the element numbers on each volume, the node numbers on each element, and the coordinates of each node. The natural frequencies and the corresponding mode shapes are extracted from the FEA solutions and used in the calculation of the FRF of the machined workpiece. The elements of the FRF, α_{ij}, can be written in terms of the natural frequencies, ω_r, and the mode shapes, $\{\varphi^r\}$, as in the following equation:

$$\alpha_{ij} = \sum_{r=1}^{n} \frac{\{\varphi_i^r\}\{\varphi_j^r\}}{\omega_r^2 - \omega^2 + i\gamma_r\omega_r^2} \quad \ldots\ldots\ldots (19)$$

where ω is the frequency for which the elements of the FRF are calculated and γ_r is the damping coefficient of the rth mode. In FRF calculations, some degrees of freedom can be eliminated if there is no modification done on them or their dynamics are not required. This is another advantage of the method proposed.

The FRFs in different machining stages are obtained by adding, step by step in reverse order, the mass removed during machining, to the finished part geometry. For a removed volume, the elements can be added one by one, or as a group, depending on the number of machining stages for which FRFs are to be determined. If the number of

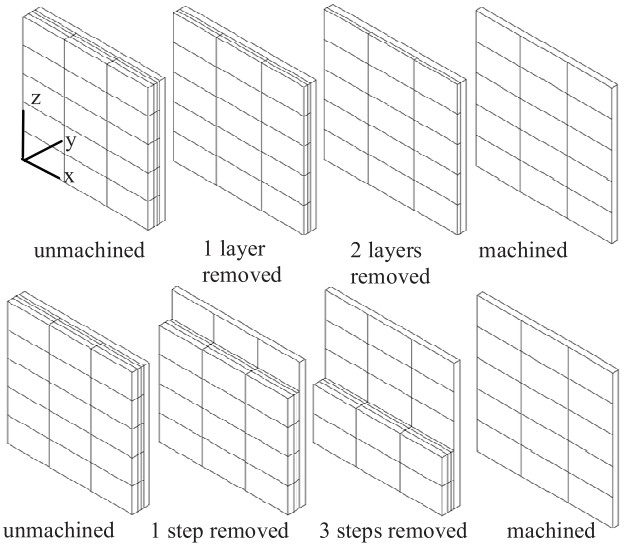

Fig. 1. Stages of layer (upper) and step removal (lower) processes.

elements added at each step is increased, the number calculation steps, and thus the computation time, decreases. However, as the number of elements added in each step increases, the size of addition matrices increases. The time for inversion and assembling the dynamics matrix becomes important as the size of the addition matrices increases. In order to minimize the computation time, for a single frequency, the structural modification procedure is applied for the different number of elements added at each step. For the whole frequency range, the number of elements that gives the minimum computation time is used.

4. Machining Stability Analysis

In this section, machining of a plate is modeled and stability analysis is performed for different cutting strategies. The dynamics of the plate is predicted for different stages of the machining cycle. Stable cutting conditions are obtained from the machining stability analyses. The effect of workpiece dynamics on productivity is investigated by comparing the results of stability analyses for different strategies.

4.1. Prediction of Workpiece FRF

A plate of Al 7075 alloy 70 mm high × 70 mm wide × 9.5 mm thick is modeled. The plate is to be machined along its thickness in order to drop the thickness from 9.5 mm to 3 mm. The geometry for the unmachined plate is shown in **Fig. 1**. The material properties are taken as modulus of elasticity of 70 GPa, Poisson's ratio of 0.33, and density of 2800 kg/m^3. Damping of the system is modeled as structural damping with a damping coefficient of 1.52%.

The workpiece under investigation can be machined using different approaches. The two main methods considered here, namely layer removal and step removal, are shown in **Fig. 1**. In layer removal, at each cutting cycle, e.g., roughing or finishing, the whole plate is brought to the same thickness by machining the plate from one end to the other. In the step removal, on the other hand, the part is brought to the final dimension at each step by applying all cutting cycles. Depending on the method selected and the cutting conditions used, part dynamics and chatter stability are affected significantly. In this case study, the machining of the plate in terms of volume removal is modeled in three steps in the *x* and *y* directions and in five steps in the *z* direction. Different cases will be analyzed representing different thickness changes, i.e., different radial depth of cuts, during machining. A total of six strategies will be analyzed (3 layer removal, 3 step removal). The removal type and the thicknesses of the layers for the strategies modeled are given in **Table 1**. The thickness of the part for Case A varies as follows: 9.5 mm, 6.5 mm, 4.5 mm, 3 mm. The volume division for case A is shown in **Fig. 1**. In order to indicate the position of machining, i.e., tool position, a coding convention is used: A_i_j_k. Here, the letter denotes the cutting strategy applied, and the numbers (i, j, k) stand for the corresponding cutting steps in the *y*, *z* and *x* directions, respectively. The step A_1_1_1 is the removal of the first element from the unmachined workpiece. Using the procedure described in section 3, the dynamics of the workpiece at each step is

Table 1. Removal types and layer thicknesses of the strategies.

Strategy	Removal type	Thickness of the 1st layer (mm)	Thickness of the 2nd layer (mm)	Thickness of the 3rd layer (mm)	Thickness of the final layer (mm)
A	layer	3.0	2.0	1.5	3.0
B	layer	4.0	1.5	1.0	3.0
C	layer	5.0	1.0	0.5	3.0
D	step	3.0	2.0	1.5	3.0
E	step	4.0	1.5	1.0	3.0
F	step	5.0	1.0	0.5	3.0

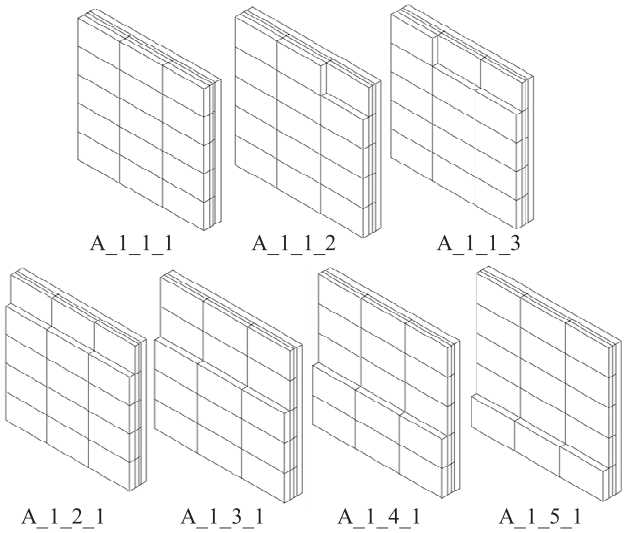

Fig. 2. Several machining steps.

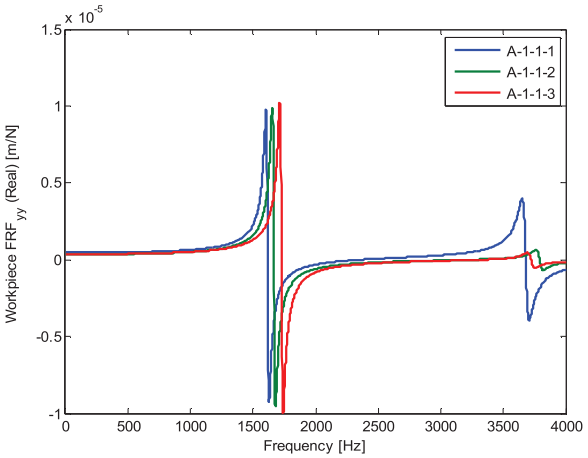

Fig. 3. Workpiece FRF_{yy} for the steps A_1_1_1, A_1_1_2, and A_1_1_3.

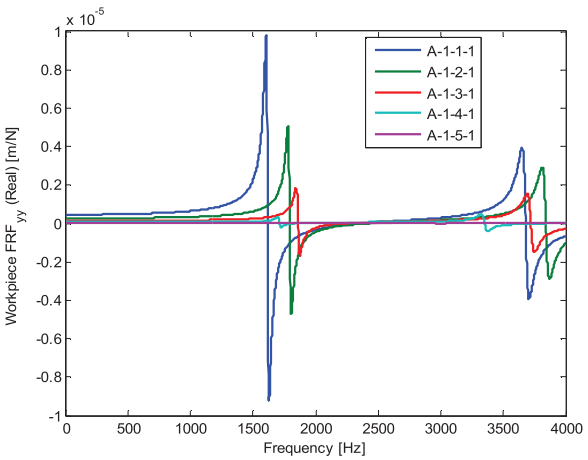

Fig. 4. Workpiece FRF_{yy} for the steps A_1_1_1, A_1_2_1, A_1_3_1, A_1_4_1, and A_1_5_1.

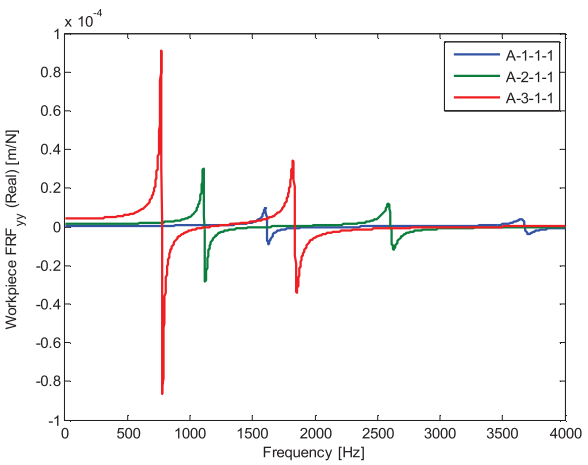

Fig. 5. Workpiece FRF_{yy} for the steps A_1_1_1, A_2_1_1, and A_3_1_1.

predicted for the point that is in contact with the tool.

The machining steps A_1_1_1, A_1_1_2, and A_1_1_3 are illustrated in **Fig. 2** whereas the corresponding FRFs in the *y* direction are shown in **Fig. 3**. It should be noted

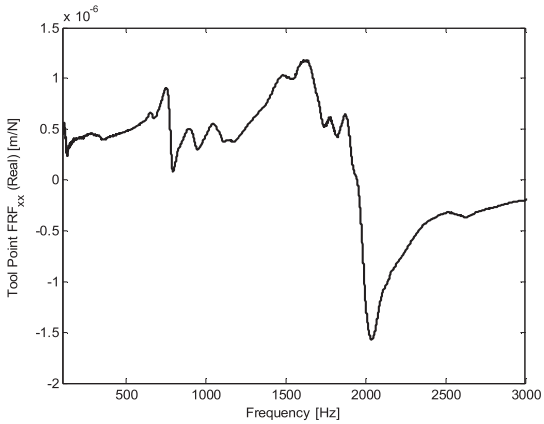

Fig. 6. Tool point FRF_{xx}.

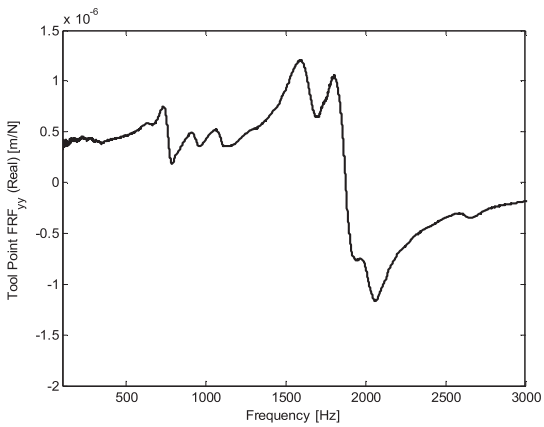

Fig. 7. Tool point FRF_{yy}.

that the workpiece is quite flexible in the *y* direction; hence FRFs are plotted for only this direction. As the machining process progresses, the tool moves down in the *z* direction. Different steps in the *z* direction, A_1_1_1, A_1_2_1, A_1_3_1, A_1_4_1, and A_1_5_1, are shown in **Fig. 2**. The corresponding FRFs in the *y* direction can be seen in **Fig. 4**. From this figure, it can be seen that the magnitude of the receptance around the fixed end of the workpiece is much lower than that near the free end, as expected.

The effect of the decreased part thickness on the part dynamics can be seen in **Fig. 5**, which shows the FRFs during the machining of the first steps of each layer. As expected, the magnitudes of the FRFs increase as the thickness of the plate is reduced.

4.2. Effects of Workpiece Flexibility on Stability Diagrams

The FRFs of the workpiece at all the steps are used in the machining stability analysis to determine the chatter-free depth of cuts. The stability analysis is done using CutPro [23], a machining simulation program developed by the Manufacturing Automation Laboratories of the University of British Columbia. Note that experimentally-obtained tool point FRFs are used in the analysis to in-

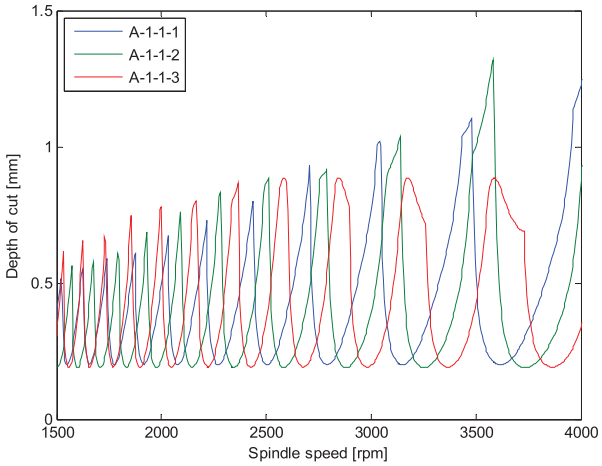

Fig. 8. Stability limits for the steps A_1_1_1, A_1_1_2, and A_1_1_3.

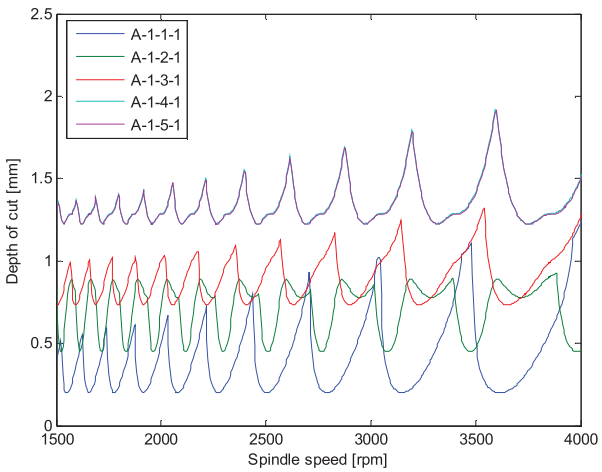

Fig. 9. Stability limits for the steps A_1_1_1, A_1_2_1, A_1_3_1, A_1_4_1, and A_1_5_1.

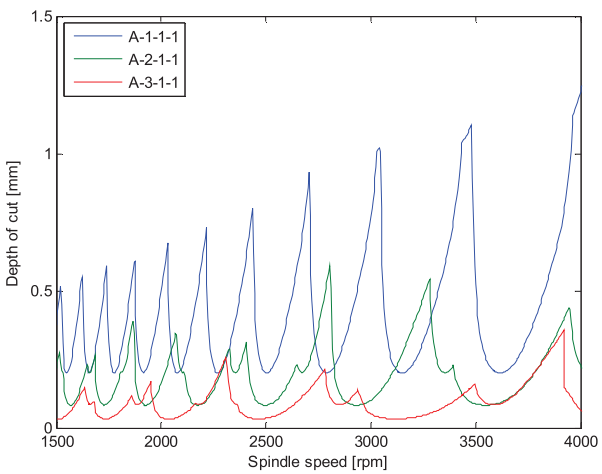

Fig. 10. Stability limits for the steps A_1_1_1, A_2_1_1, and A_3_1_1.

clude the dynamics of the spindle-holder-tool system. The FRFs, in the x and y directions, of the tool used in the analysis are given in **Fig. 6** and **Fig. 7**. The tool used is

Table 2. Stability limits (mm) for strategy A.

Step	A1_ (9.5 mm – 6.5 mm)	A2_ (6.5 mm – 4.5 mm)	A3_ (4.5 mm – 3.0 mm)
_1	0.19	0.08	0.03
_2	0.34	0.14	0.06
_3	0.73	0.37	0.15
_4	1.20	1.73	0.71
_5	1.22	1.78	2.36

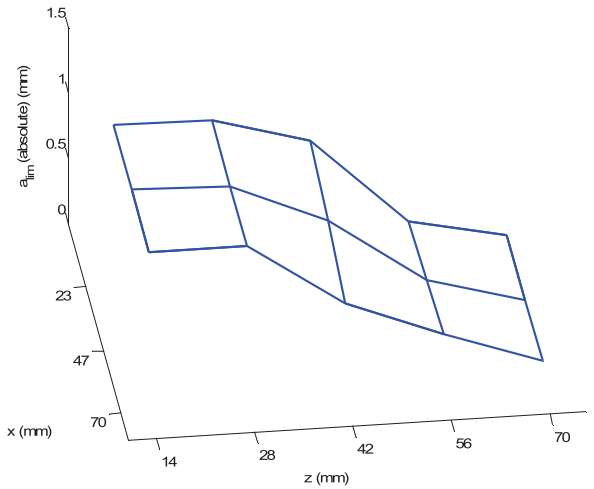

Fig. 11. Stability limits for the first layer in strategy A.

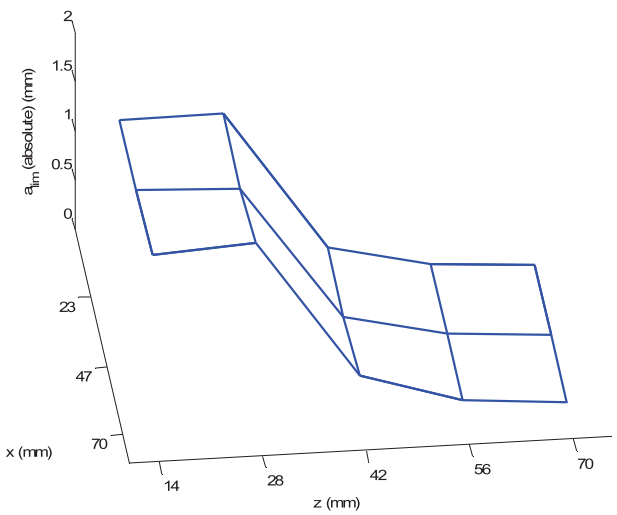

Fig. 12. Stability limits for the second layer in strategy A.

a 6 mm diameter carbide end mill with a 30° helix, four flutes, and a 5° rake angle. Average cutting force coefficients are used in the analysis. The spindle direction is clockwise and the milling mode is down-milling with a feed rate of 0.1 mm/flute.

The stability lobe diagrams obtained using CutPro for the steps A_1_1_1, A_1_1_2, and A_1_1_3 are shown in **Fig. 8**. Therefore, the diagrams shown in **Fig. 8** correspond to the variation in the stability limits as the plate is machined from one end to the other during the first layer of cut at the free end, i.e., at the beginning of ma-

Table 3. Stability limits (mm) for strategy B.

Step	B1_ (9.5 mm – 5.5 mm)	B2_ (5.5 mm – 4.0 mm)	B3_ (4.0 mm – 3.0 mm)
_1	0.17	0.06	0.03
_2	0.26	0.11	0.05
_3	0.48	0.27	0.14
_4	0.94	1.26	0.62
_5	0.94	2.27	3.48

Table 4. Stability limits (mm) for strategy C.

Step	C1_ (9.5 mm – 4.5 mm)	C2_ (4.5 mm – 3.5 mm)	C3_ (3.5 mm – 3.0 mm)
_1	0.15	0.04	0.03
_2	0.27	0.08	0.06
_3	0.45	0.20	0.15
_4	0.78	0.81	0.64
_5	0.78	3.42	6.61

Table 5. Stability limits (mm) for strategy D.

Step	D1_ (9.5 mm – 6.5 mm)	D2_ (6.5 mm – 4.5 mm)	D3_ (4.5 mm – 3.0 mm)
_1	0.19	0.22	0.28
_2	0.36	0.42	0.43
_3	1.43	0.89	1.20
_4	1.23	1.81	1.60
_5	1.22	1.78	2.36

Table 6. Stability limits (mm) for strategy E.

Step	E1_ (9.5 mm – 5.5 mm)	E2_ (5.5 mm – 4.0 mm)	E3_ (4.0 mm – 3.0 mm)
_1	0.17	0.27	0.36
_2	0.31	0.48	0.52
_3	0.67	1.39	1.35
_4	0.95	2.19	3.03
_5	0.94	2.33	3.48

chining. It can be seen from the diagrams that, although the dynamics of the workpiece do not change significantly in these steps, the lobe positions vary substantially. The stability lobe diagrams for the steps, A_1_1_1, A_1_2_1, A_1_3_1, A_1_4_1, and A_1_5_1 are plotted in **Fig. 9**. As the stiffness of the workpiece increases, so does the limiting depth of cut. The stability diagrams for the initial steps of each layer removal are shown in **Fig. 10**. The flexibility increases as the thickness is reduced and the stable depth of cut decreases.

4.3. Different Cutting Strategies

The machining of the plate is modeled with six different cutting strategies. In this section, these strategies are described in detail. The limiting stable depths of cuts and corresponding machining times are compared for all strategies. The stability limits obtained for the strategy A are given in **Table 2**. **Figs. 11** and **12** show the stability limits for the first and second layers in strategy A. As expected, the stability limits increase near the fixed end of the plate. The minimum of the three stability limits along the x direction is taken as the limiting depth of cut in the corresponding step. **Tables 3**, **4**, **5**, **6**, and **7** present the limiting depths of cut for strategies B to F, respectively.

Table 7. Stability limits (mm) for strategy F.

Step	F1_ (9.5 mm – 4.5 mm)	F2_ (4.5 mm – 3.5 mm)	F3_ (3.5 mm – 3.0 mm)
_1	0.15	0.37	0.58
_2	0.29	0.58	0.78
_3	0.56	1.55	1.64
_4	0.78	2.26	3.71
_5	0.78	3.45	6.61

Table 8. Number of passes for the steps of strategy A.

Step	A1_	A2_	A3_
_1	74	175	467
_2	42	100	234
_3	20	38	94
_4	12	9	20
_5	12	8	6
		Total	1311

Table 9. Total number of passes and machining times for six strategies considered.

Strategy	# of passes	Machining time (s)
A	1311	4588.5
B	1505	5267.5
C	1652	5782
D	387	1354.5
E	374	1309
F	348	1218

The height for each step modeled is 14 mm. The number of passes required to remove material 14 mm in height can be calculated by rounding to the first integer greater than the ratio of the height to the limiting depth of cut.

$$nop = roundup\left(\frac{h}{a_{\lim}}\right) \quad \ldots\ldots\ldots (20)$$

The number of passes required for strategy A can be calculated using the limiting depths of cut values listed in **Table 2**. **Table 8** shows the number of passes for each step for strategy A.

Table 9 gives the total number of passes for strategies A to F.

The machining time for one pass depends on the width (w) of the workpiece and the feed rate (V_f). For this case, the width is 70 mm, which is the same for all passes. The feed rate depends on the feed rate per tooth (f), the number of flutes on the cutter (N), and the spindle speed (n). The feed rate per flute is taken as 0.1 mm/flute. The number of flutes on the cutter is four and the spindle speed is 3000 rpm in the analyses. The feed rate in mm/s can be calculated as:

$$V_f = \frac{N \cdot f \cdot n}{60} = \frac{4 \cdot 0.1 \cdot 3000}{60} = 20\,\text{mm/s} \quad \ldots (21)$$

The machining time for one pass can now be obtained as:

$$t = \frac{w}{V_f} = \frac{70\,\text{mm}}{20\,\text{mm/s}} = 3.5\,\text{s} \quad . \quad . \quad . \quad . \quad . \quad . \quad . \quad . \quad . \quad (22)$$

Thus, the total machining time depends on the number of cutting steps. Note that the non-cutting times for tool positioning are neglected since they are usually small, but they may add up to be considerable if the number of steps is very high. The machining times for the six strategies are also listed in **Table 9**. It can be seen from this table that for the same radial depth of cuts, step removal strategies require much less time than the layer removal strategies. It can be concluded that step removal is superior to layer removal in terms of productivity. For layer removal, the productivity decreases if the thickness removed in the rough cut is increased and the thickness removed in the semi-finishing and finishing cuts are decreased. In the step removal strategies, increasing the thickness removed in the rough cut and decreasing those in the semi-finishing and finishing cuts, increases productivity.

5. Conclusion

The analytical procedure developed in this study is practical for the prediction of workpiece dynamics at different stages of machining. It is shown that the change in the dynamics of the workpiece may affect the stability limits substantially. Predictions of the dynamics of the workpiece are performed by the procedure developed. The productivity of different production strategies is compared using the method.

Acknowledgements

This project's funding by the Scientific and Technological Research Council of Turkey (TUBITAK) under Project number 108M340 is gratefully acknowledged.

References:

[1] S. A. Tobias, "Machine-Tool Vibration," Blackie & Son Ltd, 1965.
[2] J. Tlusty, "Manufacturing Processes and Equipment," Prentice Hall, 2000.
[3] S. A. Tobias and W. Fishwick, "Theory of Regenerative Machine Tool Chatter," The Engineer, Vol.205, pp. 199-203, 1958.
[4] J. Tlusty and M. Polacek, "The stability of Machine Tools against Self Excited Vibrations," ASME Int. Research in Production Engineering, Vol.1, pp. 465-474, 1963.
[5] H. E. Merritt, "Theory of Self-excited Machine-tool Chatter," J. of Engineering for Industry, Vol.87, pp. 447-454, 1965.
[6] F. Koenigsberger and J. Tlusty, "Machine Tool Structures," Vol.1, Pergamon Press, 1970.
[7] I. Minis and R. Yanushevsky, "A New Theorethical Aproach for the Prediction of Machine Tool Chatter in Milling," J. of Engineering for Industry, Vol.115, pp. 1-8, 1993.
[8] E. Budak and Y. Altıntaş, "Analytical Prediction of Chatter Stability in Milling – Part I: General Formulation," Trans. of the ASME, Vol.120, pp. 22-30, 1998.
[9] E. Budak and Y. Altıntaş, "Analytical Prediction of Chatter Stability in Milling – Part II: Application of the General Formulation to Common Milling Systems," Trans. of the ASME, Vol.120, pp. 31-36, 1998.
[10] T. Schmitz and R. Donaldson, "Predicting High-Speed Machining Dynamics by Substructure Analysis," Annals of the CIRP, Vol.49, No.1, pp. 303-308, 2000.
[11] T. Schmitz, M. Davies, and M. Kennedy, "Tool Point Frequency Response Prediction for High-Speed Machining by RCSA," J. of Manufacturing Science and Engineering, Vol.123, pp. 700-707, 2001.
[12] A. Ertürk, H. N. Özgüven, and E. Budak, "Analytical Modeling of Spindle–tool Dynamics on Machine Tools Using Timoshenko Beam Model and Receptance Coupling for the Prediction of Tool Point FRF," Int. J. of Machine Tools & Manufacture, Vol.46, pp. 1901-1912, 2006.
[13] E. Budak, A. Ertürk, and H. N. Özgüven, "A Modeling Approach for Analysis and Improvement of Spindle-holder-tool Assembly Dynamics," Annals of the CIRP, Vol.55, pp. 369-372, 2006.
[14] A. Ertürk, H. N. Özgüven, and E. Budak, "Effect analysis of bearing and interface dynamics on tool point FRF for chatter stability in machine tools by using a new analytical model for spindle – tool assemblies," Int. J. of Machine Tools & Manufacture, Vol.47, pp. 23-32, 2007.
[15] U. Bravo, O. Altuzarra, L. N. López de Lacalle, J. A. Sánchez, and F. J. Campa, "Stability Limits of Milling Considering the Flexibility of the Workpiece and the Machine," Int. J. of Machine Tools & Manufacture, Vol.45, pp. 1669-1680, 2005.
[16] V. Thevenot, L. Arnaud, G. Dessein, and G. Cazenave-Larroche, "Influence of Material Removal on the Dynamic Behaviour of Thin-walled Structures in Peripheral Milling," Machining Science and Technology, Vol.10, pp. 275-287, 2006.
[17] V. Thevenot, L. Arnaud, G. Dessein, and G. Cazenave-Larroche, "Integration of Dynamic Behaviour Variations in the Stability Lobes Method: 3D Lobes Construction and Application to Thin-walled Structure Milling," The International Journal of Advanced Manufacturing Technology, Vol.27, pp. 638-644, 2006.
[18] J. V. Le Lan, A. Marty, and J. F. Debongnie, "Providing Stability Maps for Milling Operations," Int. J. of Machine Tools & Manufacture, Vol.47, pp. 1493-1496, 2006.
[19] I. Mañé, V. Gagnol, B. C. Bouzgarrou, and P. Ray, "Stability-based Spindle Speed Control During Flexible Workpiece High-speed Milling," International Journal of Machine Tools & Manufacture, Vol.48, pp. 184-194, 2007.
[20] K. Weinert, P. Kersting, T. Surmann, and D. Biermann, "Modeling Regenerative Workpiece Vibrations in Five-axis Milling," Production Engineering Research and Development, Vol.2, No.3, pp. 255-260, 2008.
[21] S. Atlar, E. Budak, and H. N. Özgüven, "Modeling Part Dynamics and Chatter Stability in Machining Considering Material Removal," 1st Int. Conf. on Process Machine Interactions, Hannover, pp. 61-72, 2008.
[22] H. N. Özgüven, "Structural Modifications Using Frequency Response Functions," Mechanical Systems and Signal Processing, Vol.4, No.1, pp. 53-63, 1990.
[23] CutPro, Manufacturing Automation Lab. (http://www.malinc.com/)

Name:
Salih Alan

Affiliation:
Ph.D. Candidate, Department of Mechanical Engineering, Graduate School of Natural and Applied Sciences, Middle East Technical University

Address:
06531 Ankara, Turkey

Brief Biographical History:
2006- Graduate Student, Graduate School of Natural and Applied Sciences, Middle East Technical University

Name:
Erhan Budak

Affiliation:
Associate Professor, Faculty of Engineering and Natural Sciences, Sabanci University

Address:
Orhanli, Tuzla, 34956 Istanbul, Turkey

Membership in Academic Societies:
- International Institution of Production Engineering Research (CIRP)
- American Society of Mechanical Engineers (ASME)

Name:
H. Nevzat Özgüven

Affiliation:
Vice President, Professor of Mechanical Engineering, Middle East Technical University

Address:
06531 Ankara, Turkey

Brief Biographical History:
1985-1987 Fulbright Scholar and Visiting Professor, The Ohio State University
1992-1995 CEO and President, Turkish Cement and Earthenware Industries Co.
1998-2003 Vice President, The Scientific and Technological Research Council of Turkey

Main Works:
- "A Modal Superposition Method for Nonlinear Structures," J. of Sound and Vibration, Vol.189, No.3, pp. 315-339, 1996.
- "Analytical Modeling of Spindle-Tool Dynamics on Machine Tools Using Timoshenko Beam Model and Receptance Coupling for the Prediction of Tool Point FRF," Int. J. of Machine Tools and Manufacture, Vol.46, No.15, pp. 1901-1912, 2006.
- "Identification of Structural Non-linearities Using Describing Functions and the Sherman-Morrison Method," Mechanical Systems and Signal Processing, Vol.23, pp. 30-44, 2009.

Membership in Academic Societies:
- Fellow, American Society of Mechanical Engineers (ASME)
- Turkish Chamber of Mechanical Engineers
- Turkish Mechanical Design and Production Society
- The Fulbright Alumni Association of Turkey
- Scientific and Technical Research Foundation
- Turkish Cement Manufacturers' Association